

Comprehensive Study on the Impact of Dielectric and Magnetic Loss on Performance of a Novel Flexible Magnetic Composite Material

Li Yang¹, Lara Martin², Daniela Staiculescu¹, C. P. Wong¹, and Manos M. Tentzeris¹

¹Georgia Institute of Technology, Atlanta, GA, 30332, U.S.A.

²Motorola, Plantation, FL, 33322, U.S.A.

liyang@ece.gatech.edu

Abstract—This paper introduces a novel flexible magnetic composite material for RFID and wearable RF antennas. The critical issue of dielectric and magnetic losses combined is addressed for the first time for such a material in the UHF frequency band and is thoroughly investigated using a hybrid method including electromagnetic simulations and statistical tools. The successful implementation of the flexible magnetic composite material will enable the significant miniaturization of RF passives and antennas in UHF frequency bands, especially for applications requiring conformal modules that can be easily fine-tuned, while minimizing the decrease in performance due to losses.

I. INTRODUCTION

The inception of RFID (radio frequency identification) has enabled the contactless transfer of information without the requirement of line-of-sight association, specifically between a reader and transponders that reside on identified items. As the technology for RFID systems continuously improves and extends to structures of non-orthogonal shapes and to conformal sensors of wireless body-area networks (WBAN), there has been a need to design more “flexible” reader and tag systems. Namely, miniaturization of the transponder and ability to tune the system performance to accommodate EM (electromagnetic) absorption and interference from surrounding media, while compensating for fabrication tolerances has been one of the major priorities [1]. Three-dimensional transponder antennas that utilize wound coil inductors do make use of magnetic cores, but they are quite bulky and impractical. On the other side, magnetic materials for 2D embedded conformal planar antennas have not yet been successfully realized for standard use. This paper introduces for the first time a novel flexible magnetic composite for printed circuits and antennas, which can reap the same miniaturization and tuning benefits as the heavier and non-flexible 3D counterparts that use magnetic cores.

One of the most significant challenges for applying new magnetic materials is understanding the interrelationships of the properties of the new materials with design and performance of the specific topology (e.g. radiation pattern, scattering parameters). In previous studies, it can often be cited that the objectives of miniaturization and improved performance are tempered by the limited availability of

materials that possess the required magnetic properties, while maintaining an acceptable mechanical and conformality performance [2]. Recently, formulation of magnetic composites comprised of ferrite filler and organic matrix has been demonstrated [3]. The implication of these new magnetic materials has yet not been investigated for specific EM systems above the low MHz range. The aim of this work is to provide a basis for the co-design of materials, fabrication processes and electromagnetic structures, namely for the benchmarking case of a novel flexible magnetic composite, comprised of Co₂Z hexaferrite particles in a silicone matrix, and a UHF RFID antenna, respectively. Additionally, based on the designed antenna, the effects of dielectric and magnetic loss tangents on multiple aspects of the antenna performance are carefully investigated, so the designer knows a priori what their impact on performance is and how to account for them from the beginning of the design process.

Specifically, in this study a benchmark structure was first designed for 480 MHz in a full-wave simulator for an unfilled silicone substrate; then the ferrite particles were added and the same antenna was redesigned for 480 MHz by reducing its size, thus proving the miniaturization concept. The next step was the actual fabrication of the material and the measurement of the dielectric and magnetic characteristics, including loss. The miniaturized antenna was fabricated on the magnetic composite and its performance was measured, compared and validated along with the simulated predictions. Finally, the impact of the dielectric and magnetic loss tangents on the antenna performance was evaluated using electromagnetic simulations and statistical tools like Design of Experiments (DOE) and Response Surface Methods (RSM). Both the dielectric and the magnetic loss tangents have a significant impact on the performance, affecting directly the resonant frequency, return loss and the maximum gain at 480 MHz, with a significant change in bandwidth, but not large enough for practical applications.

II. MATERIAL DEVELOPMENT

The first step for this work was to develop a magnetic composite that provides the advantage of low-temperature processing for compatibility with common organic substrate

processes, flexibility, and high adhesion requirements. Additionally, the composite dielectric loss can affect circuit performance, and low dielectric loss would be targeted. Dielectric constant variation can also affect the circuit performance and should also be monitored. The matrix materials considered candidates for this proposed work included silicone and benzocyclobutene (BCB). Silicone provides reasonable viscosities required for good filler mixing during processing, and provides the properties of flexibility and, for some formulations, good adhesion.

After careful analysis, the matrix material choice was made for Dow Corning Sylgard 184 silicone. The electrical parameters of the unfilled silicone, used in the initial antenna design, are $\epsilon_r = 2.65$ and $\tan\delta_e = 0.001$. The choice for the magnetic composite was Co_2Z hexaferrite powder supplied by Trans-Tech. A 40 vol% ferrite paste was produced with a mixer at 240 rpm and 110°C for 30 minutes. The paste was transferred into a flat mold and vacuum cured with a hold confirmed to occur at about 121°C for 80 minutes to produce a 1.21 mm thick substrate.

The material was measured using an HP4291A impedance analyzer to obtain complex permittivity (ϵ^*) and permeability (μ^*) (real and imaginary parts) with material fixtures 16453A for ϵ^* and 16454A for μ^* over the frequency range of 1MHz to 1.8GHz. There were 5 measurements taken for each ϵ_r , μ_r , $\tan\delta_e$ and $\tan\delta_m$. The summary statistics, including the mean and 95% C.I. (confidence intervals) for ϵ_r , μ_r , $\tan\delta_e$ and $\tan\delta_m$ of the ferrite composite at 480 MHz are given in TABLE I. Based on these results, the values used in the model were $\epsilon_r = 7.14$, $\mu_r = 2.46$, $\tan\delta_e = 0.0017$ and $\tan\delta_m = 0.039$.

TABLE I

MEAN AND 95% CONFIDENCE INTERVALS FOR ϵ AND μ MEASUREMENTS OF FERRITE COMPOSITE AT 480 MHz

	Mean	Lower CI	Upper CI
ϵ_r	7.142	7.083	7.201
μ_r	2.463	2.457	2.468
$\tan\delta_e$	0.0017	0.0005	0.0028
$\tan\delta_m$	0.0391	0.0358	0.0424

III. ANTENNA DESIGN AND MEASUREMENT

The demand for flexible RFID tags has rapidly increased due to the requirements of automatic identification in item-level tracking, as well as for the deployment of wearable biomonitoring devices. The UHF RFID band varies in frequency, power levels, number of channel and sideband spurious limits of the RFID readers signal, depending on the application and the area of operation, such as 866-956MHz in North America/Europe for EPC GEN2 item-level tracking and the lower band around 400MHz for bio-applications.

Another challenge concerns the miniaturization of the dimensions of the RFID tags for flexible operation. The free space wavelength at 480MHz is 692mm. An RFID tag that

has a compact size is becoming more of a necessity, for example, in the implementation of an RFID-enabled wristband tags or sensors for wireless health monitoring in hospitals.

To achieve these design goals, a folded bow-tie meander line dipole antenna was designed and fabricated on the characterized magnetic composite material substrate. The RFID prototype structure is shown in Fig. 1 along with dimensions, with the IC placed in the center of the shorting stub arm. Fig. 2 shows a picture of the fabricated antenna on the magnetic composite.

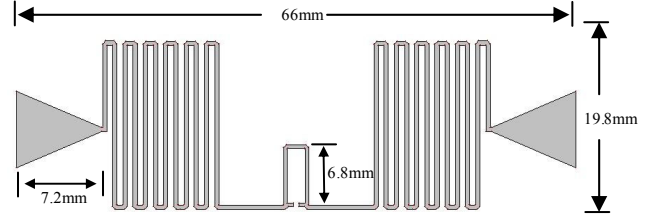


Fig. 1. Configuration of the RFID tag module on magnetic composite substrate.



Fig. 2. Picture of fabricated antenna for various conformal applications, like wireless health monitoring and pharmaceutical drug bottle tracking.

The initial structure was designed for the lower end of the UHF spectrum and was modeled using Zeland IE3D full-wave EM software. The initial substrate was pure silicone ($\epsilon_r = 2.65$ and $\tan\delta = 0.001$) of 1.21mm thickness. Then the same dimensions of the antenna were maintained for the magnetic composite material and the shift in the resonant frequency was observed. The Return Loss plot is shown in Fig. 3, demonstrating a frequency down shifting of 20% with increased magnetic permeability, which verifies the miniaturization concept. The radiation pattern of the miniaturized antenna is almost uniform (omnidirectional) at 480MHz with gain around -4.5 dBi.

The fabricated antenna return loss was then compared with the IE3D simulation and the result in Fig. 4 shows very good agreement. A GS 1000 μm pitch probe was used for the on-wafer measurements. In order to minimize backside reflections of this type of antenna, the fabricated antenna was placed on a custom-made probe station using high density polystyrene foam with low relative permittivity of value 1.06 resembling that of the free space. The calibration method used was short-open-load-thru (SOLT).

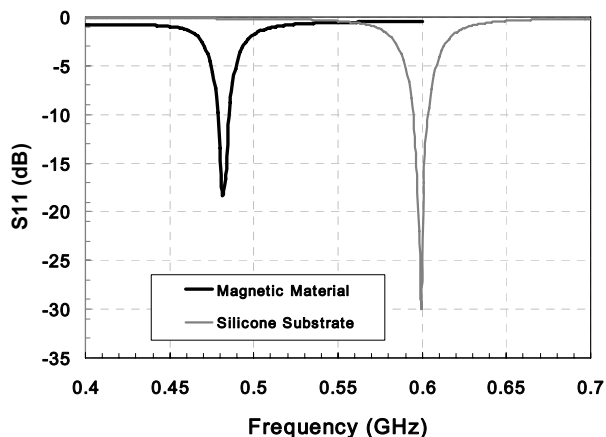


Fig. 3. Measured results for the miniaturized antenna, compared with the antenna performance on silicone substrate.

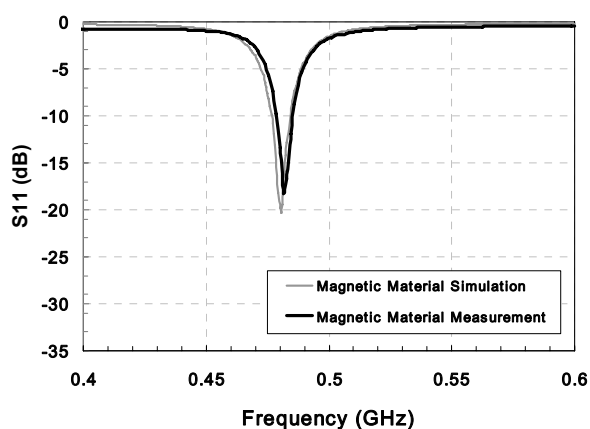


Fig. 4. Simulations validated with measurements.

IV. STATISTICAL ANALYSIS AND OPTIMIZATION

One of the most critical factors in the magnetic composite fabrication was the control of loss, so a careful analysis of the impact of both the dielectric and magnetic performance based on the fabrication variability was necessary.

The methodology used in the optimization of the antenna with respect to losses is presented as a flowchart in Fig. 5. First, DOE is performed to develop the first order statistical model, including both loss tangents, dielectric and magnetic. Then, the model is checked for ultimate lack of fit, such as, if curvature might be present in the output response. If curvature in the response is detected, the analysis is extended to additional axial points indicated by the RSM method, which can account for curvature through second-order model development. Usually, these second-order models are reasonable approximations of the true functional relationship over relatively small regions. Once validated using statistical diagnostic tools, the models approximate the actual system within the defined design space.

The experimentation method chosen for the first-order statistical model is a full factorial DOE with center points [5]. The factorial designs are used in experiments involving several factors where the goal is the study of the joint effects of the factors on a response and the elimination of the least important ones from further optimization iterations. The 2^k factorial design is the simplest one, with k factors at 2 levels each. It provides the smallest number of runs for studying k factors and is widely used in factor screening experiments [5]. Center points are defined at the center of the design space and enable investigating validity of the model, including curvature in the response, and account for variations in the fabrication process of the structure. Since the statistical models are based on deterministic simulations, the variations of the center points were statistically simulated assuming a 3σ process with a $\pm 2\%$ tolerance for both $\tan\delta_e$ and $\tan\delta_m$.

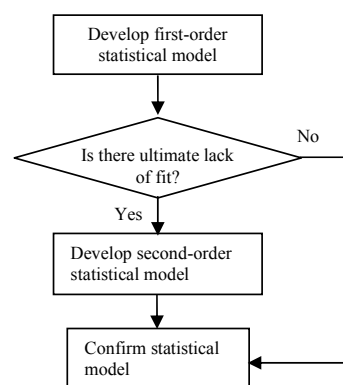


Fig. 5. Procedure for statistical model development

In this case, since we have two input variables, a 2^2 full factorial DOE was performed for the first-order statistical model, with the following 4 output variables as the antenna performance figures of merit: resonant frequency f_{res} , minimum return loss RL , maximum gain at 480 MHz G , and the 10 dB bandwidth BW . The ranges of the input variables are presented in Table II.

TABLE II.
RANGES FOR THE INPUT VARIABLES

Variable	Low value “-”	High value “+”	Center point
$\tan\delta_e$	0.00136	0.00204	0.0017
$\tan\delta_m$	0.0312	0.0468	0.039

The first order models showed curvature in all of the responses, and RSM was needed for the second-order statistical model. Validation of the models was investigated, with all but the BW validated for the normality assumption, and the equal variance was validated for RL and G , but not for f_{res} and BW . The four models are given by the following:

$$f_{res} (MHz) = 480.47 - 0.024 \left(\frac{\tan \delta_{\mu} - 0.039}{0.0078} \right) - 0.013 \left(\frac{\tan \delta_{\mu} - 0.039}{0.0078} \right)^2$$

$$RL (dB) = -20.34 + 0.18 \left(\frac{\tan \delta_{\epsilon} - 0.0017}{0.00034} \right) + 2.48 \left(\frac{\tan \delta_{\mu} - 0.039}{0.0078} \right) - 0.062 \left(\frac{\tan \delta_{\mu} - 0.039}{0.0078} \right)^2 - 0.43 \left(\frac{\tan \delta_{\epsilon} - 0.0017}{0.00034} \right) \left(\frac{\tan \delta_{\mu} - 0.039}{0.0078} \right)$$

$$G (dBi) = -4.57 - 0.019 \left(\frac{\tan \delta_{\epsilon} - 0.0017}{0.00034} \right) - 0.26 \left(\frac{\tan \delta_{\mu} - 0.039}{0.0078} \right) - 0.0044 \left(\frac{\tan \delta_{\mu} - 0.039}{0.0078} \right)^2 + 0.0005 \left(\frac{\tan \delta_{\epsilon} - 0.0017}{0.00034} \right) \left(\frac{\tan \delta_{\mu} - 0.039}{0.0078} \right)$$

$$BW (MHz) = 7.69 + 0.0000088 \left(\frac{\tan \delta_{\epsilon} - 0.0017}{0.00034} \right) + 0.038 \left(\frac{\tan \delta_{\mu} - 0.039}{0.0078} \right) - 0.031 \left(\frac{\tan \delta_{\mu} - 0.039}{0.0078} \right)^2 - 0.005 \left(\frac{\tan \delta_{\epsilon} - 0.0017}{0.00034} \right) \left(\frac{\tan \delta_{\mu} - 0.039}{0.0078} \right)$$

The models offer the capability to optimize the antenna performance with respect to either figure of merit or both simultaneously allocating any weight factors to each one of them. The optimization goals chosen in this case were a specific f_{res} of 480.47MHz (center point value), maximum gain G , minimum return loss RL and maximum bandwidth BW , all with equal weight. The surfaces for the four figures of merit as a function of the optimizing parameters are presented in Fig. 6, indicating the curvature in the models. The values that satisfied the four optimization conditions within the ranges presented in TABLE II were $\tan \delta_{\epsilon} = 0.00136$ and $\tan \delta_{\mu} = 0.032427$, leading to the optimized values of the four figures of merit of $f_{res} = 480.48$ MHz, $RL = -22.97$ dB, $G = -4.32$ dBi and $BW = 7.63$ MHz. The models indicate that the resonant frequency decreases with the losses, as the gain and the return loss obviously degrade. For the bandwidth, although the model is significant and shows an increase of the bandwidth with losses, the absolute numbers in the RSM vary only between 7.61 and 7.7 MHz, which is not a large difference for practical applications.

magnetic composite material to the miniaturization of RFID antennas considering geometric, material, and fabrication parameters, with an emphasis on dielectric and magnetic loss. This approach has been applied to the design of a benchmarking conformal RFID tag module and has enabled the assessment of implications that materials have on this design, specifically that the antenna is miniaturized by using the magnetic composite versus pure silicone. A real composite material has been fabricated and the performance of the miniaturized antenna predicted using the models. The impact of the losses on the antenna performance was very thoroughly investigated and it was found that, in the chosen ranges, the losses affect the resonant frequency, the return loss, maximum gain, and bandwidth, although change in bandwidth is not large for practical applications. This is a demonstration of a flexible magnetic composite proven for the 480 MHz bandwidth, that makes it usable for small size, lightweight conformal applications like wireless health monitoring in pharmaceuticals, hospital, ambulance and home-based patient care, as well as for wearable electronics.

ACKNOWLEDGMENT

The authors wish to acknowledge the NSF ECS-0313951, the Georgia Electronic Design Center (GEDC). Special thanks to Dr. Michael D. Hill and Barry W. Treadway of Trans-Tech, Inc., in Adamstown, Maryland, and David J. Meyer and Haiying Li of Motorola in Plantation, Florida.

REFERENCES

- [1] "Magnetic Materials for RFID," TechnoForum 2005, TDK, http://www.tdk.co.jp/tf2005/pdf_e/2f0215e.pdf.
- [2] N. Das and A. K. Ray, "Magneto Optical Technique for Beam Steering by Ferrite Based Patch Arrays," *IEEE Transactions on Antennas and Propagation*, vol. 49, no. 8, August (2001); pp. 1239-1241.
- [3] H. Dong, F. Liu, Q. Song, Z.J. Zhang, C. P. Wong, "Magnetic Nanocomposite for High Q Embedded Inductor," *IEEE International Symposium and Exhibition on Advance Packaging Materials: Process, Properties, and Interfaces*, Atlanta, Georgia, March (2004); pp. 171-174.
- [4] J. Neter *et al*, "Applied Linear Statistical Models", 4th Ed., The McGraw-Hill Companies, Chicago, 1996.

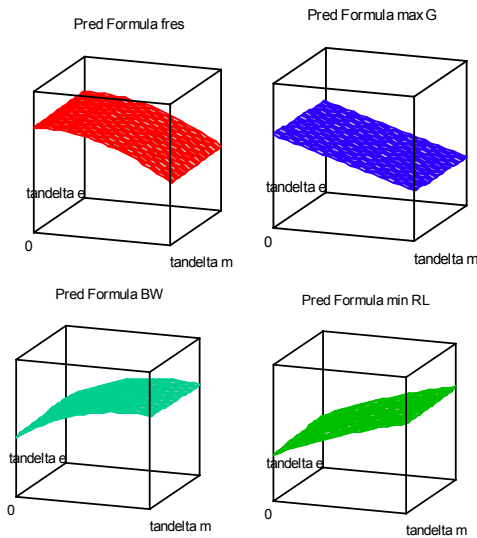


Fig. 6. Surfaces of possible solutions for outputs.

V. CONCLUSIONS

A combination of EM simulation, statistical tools, and measurements has been used to investigate the impact of a